



HAL
open science

Degradation dynamics and processes associated with the accumulation of *Laminaria hyperborea* (Phaeophyceae) kelp fragments: an in situ experimental approach

Florian de Bettignies, Patrick Dauby, François Thomas, Angélique Gobet, Ludovic Delage, Olivier Bohner, Stéphane Loisel, Dominique Davoult

► To cite this version:

Florian de Bettignies, Patrick Dauby, François Thomas, Angélique Gobet, Ludovic Delage, et al.. Degradation dynamics and processes associated with the accumulation of *Laminaria hyperborea* (Phaeophyceae) kelp fragments: an in situ experimental approach. *Journal of Phycology*, 2020, 56 (6), pp.1481-1492. 10.1111/jpy.13041 . hal-03035135

HAL Id: hal-03035135

<https://hal.science/hal-03035135>

Submitted on 2 Dec 2020

HAL is a multi-disciplinary open access archive for the deposit and dissemination of scientific research documents, whether they are published or not. The documents may come from teaching and research institutions in France or abroad, or from public or private research centers.

L'archive ouverte pluridisciplinaire **HAL**, est destinée au dépôt et à la diffusion de documents scientifiques de niveau recherche, publiés ou non, émanant des établissements d'enseignement et de recherche français ou étrangers, des laboratoires publics ou privés.



**DEGRADATION DYNAMICS AND PROCESSES ASSOCIATED
WITH THE ACCUMULATION OF KELP FRAGMENTS: AN IN
SITU EXPERIMENTAL APPROACH**

Journal:	<i>Journal of Phycology</i>
Manuscript ID	JPY-19-156-ART
Manuscript Type:	Regular Article
Date Submitted by the Author:	31-Jul-2019
Complete List of Authors:	de Bettignies, Florian; Station Biologique de Roscoff, UMR7144 AD2M; Sorbonne University, Dauby, Patrick; Université de Liège Faculté des Sciences, Systematics and Animal Diversity Thomas, François; Station Biologique de Roscoff, UMR8227 LBIMM Gobet, Angélique; Station Biologique de Roscoff, UMR8227 LBIMM Delage, Ludovic; Station Biologique de Roscoff, UMR8227 LBIMM Bohner, Olivier; Station Biologique de Roscoff, UMR7144 AD2M Loisel, Stéphane; Station Biologique de Roscoff, UMR7144 AD2M Davoult, Dominique; Station Biologique de Roscoff, UMR7144 AD2M
Keywords:	kelp, Macroalgae, Phaeophyceae
Alternate Keywords:	Degradation, Metabolism, Composition, Bacteria, Organic Matter

20 **Title page word count:** 95

21 **Abstract word count:** 243

22 **Main body word count:** 5189

23 **Figure & Table legends:** 262

24 **Acknowledgements:** 88

25 **Number of references (word count):** 60 (1853)

26 Authors' contributions: FdB, PD and DD conceived the ideas and designed the study. FdB, OB,
27 FT, AG and LD processed the samples. FdB and DD analysed the data. FdB, DD, OB and SL
28 collected the data. FdB and DD wrote the first draft and PD, FT, AG and LD extensively
29 contributed to the corrections.

30 ABSTRACT:

31 A high proportion of the kelp *Laminaria hyperborea* production is exported from kelp forests
32 following seasonal storm events or natural annual old blades loss. Drift kelp is transported and
33 can accumulate temporarily in benthic subtidal habitats. We investigated the degradation
34 processes of *L. hyperborea* in a low subtidal (-8 m) sandy bottom ecosystem by setting up a six-
35 month cage experiment to simulate drift kelp accumulation. During the degradation process, we
36 compared changes in biomass, nutritional quality (C:N ratio), respiration, quantum efficiency of
37 photosystem II (Fv/Fm) and chemical defence concentrations. We found that biomass
38 decomposition started after 2 weeks and followed a classic negative exponential pattern. Half of
39 the biomass had degraded after 8 weeks and only 16% of the initial biomass remained after 25
40 weeks. The degradation process seemed to reach a critical step after 11 weeks, with an increase in
41 respiration rate and phlorotannin concentration. These results likely reflect an increase in
42 bacterial activity and a weakening of the kelp cell wall. Surprisingly, the large fragments
43 remained visually intact after 25 weeks of degradation, and photosystems were still responding
44 correctly to light stimuli, indicating that photosynthesis appears to persist over time in fragments.
45 Reproductive tissues appeared after 4 months of degradation, showing a capacity to maintain the
46 reproductive function. Our results indicate that degrading kelps degrade slowly and because they
47 maintain their major functions (photosynthesis, reproduction, etc.) and accumulate on adjacent
48 ecosystems may play a long-term ecological role in coastal ecosystem dynamics.

49 KEY INDEX WORDS: Kelp, Degradation, Metabolism, Composition, Bacteria, Organic Matter

50

51 1. INTRODUCTION

52 Degradation is a key process in the organic matter cycle and drives biogenic ecosystems in
53 terrestrial and marine environments. Degradation includes the decomposition (biomass
54 breakdown) of primary producers and litter, and leads to remineralisation driven by micro- and
55 macroorganisms that colonise the organic matter (Pandey et al., 2007; Polyakova and Billor,
56 2007; Rees, 2001). Litterfall amounts and dynamics are closely related to the growth and
57 productivity of source ecosystems (Matala et al., 2008; Miller, 1984). In terrestrial ecosystems,
58 each plant species has a specific decomposition rate depending on its lignin constituents and
59 nitrogen content (Hendricks and Boring, 1992; Wesemael and Veer, 1992), but also depending on
60 environmental conditions (litterfall moisture, temperature) (Krishna and Mohan, 2017). In
61 contrast to terrestrial systems, marine environments are highly dynamic and variable in terms of
62 water motion and environmental conditions, especially in coastal systems. Despite this major
63 difference, accumulations of seagrass (Cardona et al., 2007; Pergent et al., 1994) and macroalgae,
64 such as kelps, are observed on the seafloor from deep (Filbee-Dexter and Scheibling, 2014;
65 Vetter, 1994) to subtidal (Tzetlin et al., 1997) and intertidal habitats (Bustamante et al., 1995).
66 Macroalgal accumulations are comparable to terrestrial litterfall, modifying the recipient
67 substratum and being influenced by associated micro- and macroorganisms and environmental
68 conditions.

69 Among macroalgae, kelps are major components of marine ecosystem functioning in temperate
70 and sub-polar regions around the globe. Kelp forests play a key role in coastal environments as
71 habitat-forming species, wave-energy dissipaters and major actors in the carbon cycle (Christie et
72 al., 2003; Leclerc et al., 2015; Teagle et al., 2017). As highly productive primary producers, kelps
73 assimilate carbon dioxide to produce organic matter via photosynthetic processes (Bartsch et al.,
74 2008). Kelps are fast growing producers that accumulate a high quantity of organic matter (>1 kg

75 C.m².yr⁻¹, Krumhansl and Scheibling, 2012a). A high proportion of this biomass is exported
76 during blade erosion, natural mortality or dislodgment related to strong hydrodynamic events (de
77 Bettignies et al., 2013; Krumhansl and Scheibling, 2012; Pessarrodona et al., 2018). Detrital
78 material can drift across habitats and, when hydrodynamic conditions are suitable, accumulates in
79 benthic habitats. Accumulation of kelp detritus can strongly influence the recipient trophic food
80 web (Krumhansl and Scheibling, 2012b; Tzetlin et al., 1997). Globally, 82% of annual kelp
81 production is exported, becoming detrital subsidies (de Bettignies et al., 2013; Krumhansl and
82 Scheibling, 2012a). Within kelp forests, detrital material contributes to the particulate organic
83 matter (POM) pool and plays an important role in trophic food webs (Leclerc et al., 2013).

84 *Laminaria hyperborea* (Laminariales) is a dominant kelp species in the North-East Atlantic,
85 distributed from Portugal to Norway (Steneck et al., 2002). In Brittany, France, this species
86 dominates subtidal rocky ecosystems from 0 to 30 m below chart datum. Growth of *L.*
87 *hyperborea* sporophytes occurs in winter and spring, ceasing in July (Lüning, 1979). In spring, *L.*
88 *hyperborea* retains the old blade from the previous year during the rapid growth of the new blade.
89 Between April and May, the old blade is shed from the fast-growing new blade. The release of
90 the previous season's growth contributes significantly to the total detritus production
91 (Pessarrodona et al., 2018). *L. hyperborea* detritus represents a trophic resource that connects
92 habitats, becoming increasingly accessible to consumers as it degrades (Norderhaug et al., 2003).

93 In some areas, within kelp forest grazers may only consume a small fraction of kelp productivity
94 (Hereward et al., 2018), whereas in other systems, grazing by sea urchins is a major process
95 structuring *L. hyperborea* forests (Ling et al., 2014). In Brittany, grazers appear to consume a
96 very small fraction of the *L. hyperborea* production, with a high proportion being exported to

97 adjacent ecosystems. Therefore, the degradation kinetics of *L. hyperborea* detritus and its impact
98 on recipient ecosystems appear to be key elements in ecosystem functioning.

99 In the present study, we explored *L. hyperborea* decomposition dynamics and the degradation
100 process in an *in situ* six-month experimental approach using litterfall cages to simulate drift kelp
101 accumulation on a sandy bottom ecosystem. To investigate the kinetics of detritus biomass
102 decomposition, we monitored multiple parameters such as carbon (C) and nitrogen (N) content,
103 phlorotannin concentration, photosynthesis, respiration and abundance of cultivable alga-
104 associated bacteria. We tested whether *L. hyperborea* degradation was a quick process, with total
105 decomposition of biomass after several months. The parameters were thus expected to vary
106 accordingly, with a decrease in the C:N ratio (often related to nutritional quality and palatability),
107 a change in tissue phlorotannin concentration (related to stress and defence mechanisms) and a
108 decrease in the major functions such as production, respiration and reproduction.

109 2. MATERIALS AND METHODS

110 2.1. Study site

111 The present study was conducted near Roscoff, in the Bay of Morlaix, along the north-western
112 coast of Brittany, France. The bay is composed of numerous rocky reefs supporting high *L.*
113 *hyperborea* biomass stock (Gorman et al., 2013), separated by large areas of fine and soft
114 sediments that temporarily receive accumulations of drift kelp (personal observation). The
115 experimental site (Guerhéon: 48°42'33.78" N, 003°57'12.36" W) was located in a semi-enclosed
116 part of the bay, protected from the prevailing westerly winds, but exposed to north and easterly
117 winds that occasionally occur during spring and summer anticyclonic conditions. The site
118 substratum was characterised by a mixture of coarse sand and shell fragments at 4.5 m depth

119 below chart datum (9 m average depth) and distant by ca. 100 m from rocky reefs covered with
120 kelp forests.

121 2.2. Experimental design

122 We set up an *in situ* cage experiment to investigate the degradation dynamics of *L. hyperborea* on
123 a subtidal sandy ecosystem (Figure 1). The study was conducted from 18 April to 5 October 2017
124 (5.5 months). The experiment was deployed in April to mimic the storm events that typically
125 occur during spring and break up and dislodge part of the kelp population and increase the
126 amount of detrital kelp deposits. In this experiment, we chose to simulate storm damage on kelps
127 that are losing their old frond and studied the degradation process on the physiologically active
128 new blades.

129 During scuba dives, we randomly collected whole adults of *L. hyperborea* with a 80-90 cm stipe
130 length corresponding to 5-6 year-old kelps (Sheppard et al., 1978) without visible signs of
131 degradation from a natural population on a rocky reef close to the experimental site. Kelp
132 samples were kept in seawater and brought back to the harbour where they were processed within
133 2 hours. New blades were cut once in length and once in width. This method gave different
134 fragment sizes similar to those found in the field. Fragments from two individuals were pooled
135 and weighed with a digital spring scale (Amiaud Durer, 40 kg, ± 10 g) for a mean \pm SD wet mass
136 of 911 ± 105 g. Batches were gently packed and randomly allocated to custom-built numbered
137 plastic litterfall cages ($30 \times 25 \times 10$ cm, 1 cm mesh) made of hard plastic mesh used in oyster
138 farming. The quantity of algal material in the cage corresponded a 10 cm thick accumulation of
139 kelp fragments with a three-dimensional structure, as previously observed during prospection
140 dives. A total of 35 litterfall cages were prepared with new blades, kept in seawater and quickly
141 immersed on the experimental site by divers. To compare the degradation kinetics between

142 young and old blades, five litterfall cages were filled with old blade fragments following the
143 same procedure. Cages were attached on four anchored chain lines arranged parallel to each
144 other, forming a relatively continuous rectangle of accumulated fragments (Figure 1). We
145 checked the cages throughout the experiment to ensure that they were not buried in sediment. At
146 each sampling time (2, 4, 6, 11, 15, 20, 24 weeks), five replicates of new-blade litterfall cages
147 were randomly collected. Additionally, one old-blade litterfall cage was randomly collected at
148 five sampling dates (4, 6, 11, 15, 20 weeks). Cages were collected with caution using 1 mm mesh
149 bags, for 3 of them incubated for *in-situ* respirometry measurements, brought to the surface,
150 transported within site seawater to the laboratory for bacterial sampling before any other
151 processing. Cages were then kept in the dark in a continuous-flow seawater tank with constant air
152 bubbling until laboratory measurements (performed within 24 h).

153 2.3. Field measurements

154 2.3.1. *Environmental parameters*

155 An array of environmental sensors were deployed on the experimental site to measure
156 temperature, light intensity and water motion over the six-month period. Temperature and light
157 intensity were measured with the same sensor (HOBO Pendant Temperature/Light Weatherproof
158 Pendant Data Logger 16K) attached on a plate fixed horizontally on a threaded rod at 20 cm from
159 a concrete block. Relative water motion was measured with an accelerometer (HOBO Pendant G
160 Data Logger) attached to a small dome-shaped buoy. The buoy was tethered to the seabed with a
161 0.75 m rope clamp on a different concrete block according to (Bennett et al., 2015) design. These
162 sensors were deployed at 3 m from the experimental system and a replicate set was deployed to
163 offset any sensor failure. At each sampling time, sensors were changed or cleaned to prevent too
164 much fouling on the rope or on the sensor. All sensors were programmed to take one

165 measurement every five minutes. For each sampling time, the maximum, minimum and average
166 values of the previous week were measured for temperature and relative water motion (RWM).
167 Only the daily average was used for light. For the RWM, only two channels were used (x, y) to
168 account for horizontal acceleration (cf. H₂O motion V2 design; Evans and Abdo (2010). The
169 sensor was set to record acceleration (m.s⁻²). The RWM was standardised and measured as the
170 vector sum for all pairwise recordings according to (Evans and Abdo, 2010) methodology.

171 2.3.2. *In situ litterfall cage respiration rate*

172 Litterfall cage respiration rates were measured underwater at the experimental site during each
173 collection time on three of the five randomly collected new-blade litterfall cages. Three benthic
174 chambers were set up *in situ* by scuba divers. The custom-built incubation chambers (Ouisse et
175 al., 2014) were composed of a base to isolate the measured sample from the sediment, a Plexiglas
176 cylinder and dome sealed by a clamp system enclosing a total volume of 26.2 L of seawater.
177 Chambers were assembled ensuring no air bubbles remained inside and seawater was mixed
178 within the chambers with an autonomous stirrer. The three selected cages harvested in their mesh
179 bags were allocated to one benthic chamber each. Cages were incubated in the benthic chambers
180 covered by black tarpaulins to ensure darkness for 30 min. A sample of seawater was collected
181 from each chamber by using 100 mL syringes at the beginning and at the end of the incubation
182 (two-point method) and directly brought to the surface after sampling. Dissolved oxygen
183 concentration was immediately measured on the boat using a portable multi-meter (HQ40d,
184 Hach®, Loveland, CO, USA) coupled with a luminescent/optical dissolved oxygen probe
185 (Intellical™ LDO101, Hach®, accuracy ± 0.2 mg.L⁻¹). Litterfall cage respiration rate was
186 estimated from the difference between initial and final oxygen (O₂) concentrations after being
187 corrected for temperature change. Respiration was expressed as O₂ consumption in mg O₂.cage⁻¹

188 $l \cdot h^{-1}$, to allow comparisons between litterfall cages over time. Although continuous O_2
189 measurement is recommended, measurement only at the beginning and at the end of the
190 incubation is considered acceptable to obtain a correct measurement of community metabolism
191 for short incubations (Ouisse et al., 2014).

192 2.4. Laboratory measurements

193 In the laboratory, the contents of each cage were placed in the corresponding 1 mm mesh bag,
194 and kept in the dark in a large tank with running seawater. For each sample and measurement,
195 bags were opened in the laboratory and directly brought back to the seawater tank after
196 processing.

197 2.4.1. *Cultivable bacteria counts*

198 For each litterfall cage, 10 pieces of algal tissue were collected using a stainless steel punch (13
199 mm diameter) sterilised by flaming with 70% ethanol. Algal pieces were transferred to 20 mL of
200 sterile saline solution (for 1 L: 24.7 g NaCl, 6.3 g $MgSO_4 \cdot 7H_2O$, 4.6 g $MgCl_2 \cdot H_2O$, 0.7 g KCl),
201 stored on ice and returned within 1 h to the laboratory for further processing. The 10 algal pieces
202 from one cage were rinsed twice in 20 mL sterile saline solution and homogenised in a single
203 batch for 1 min at 8000 rpm in 20 mL sterile saline solution using a T25 Ultra-Turrax blender,
204 followed by 1 min of vortex agitation at maximum speed. Serial dilutions (from 10^{-1} to 10^{-4}) of
205 homogenates were prepared in sterile saline solution. Then, 100 μ L of the dilutions were spread-
206 plated in duplicate and incubated at 20°C for 7 days. Four media were used to screen cultivable
207 bacteria presenting different functions. The Zobell agar medium (for 1 L: 5 g tryptone, 1 g yeast
208 extract, 15 g agar in natural seawater), a highly nutritive medium, was used as a proxy of the total
209 community of cultivable bacteria. Bacteria resisting high concentrations of iodine, one of the

210 defence compounds released by kelps (Verhaeghe et al., 2008), were screened on a Zobell agar
211 medium supplemented with 100 mM KI. Bacteria were also grown on a minimum medium
212 solidified with Phytigel (for 1 L: 24.7 g NaCl, 6.3 g MgSO₄·7H₂O, 4.6 g MgCl₂·H₂O, 2 g NH₄Cl,
213 0.7 g KCl, 0.6 g CaCl₂, 200 mg NaHCO₃, 100 mg K₂HPO₄, 1X vitamin mix, 20 mg FeSO₄·7
214 H₂O, 20 g Phytigel) (Thomas et al., 2011) and supplemented with 4 g.L⁻¹ alginate, a
215 polysaccharide accounting for 10-45% of the dry mass of brown algal cell wall (Kloareg and
216 Quatrano, 1988) or 4 g.L⁻¹ mannitol, one of the main carbon storage forms in brown algae
217 (Iwamoto and Shiraiwa, 2005). (Technical) duplicate measurements were averaged and results
218 were expressed as the number of colony-forming units per unit area of algal tissue (cfu.cm⁻²). The
219 detection limit was 75 cfu.cm⁻². The proportion of iodine-resistant cultivable bacteria was
220 estimated as the ratio of counts obtained on KI-supplemented Zobell agar compared to counts
221 obtained on Zobell agar.

222 *2.4.2. Phlorotannin assay*

223 For each cage, 10 disks of 28 mm diameter were randomly cored on kelp fragments and stored at
224 -20°C before processing. Phlorotannin extraction was performed using an method adapted from
225 Li et al. (2017) and Koivikko et al. (2007). Frozen samples were stored overnight at -80°C and
226 freeze-dried for 24 h. First, 100 mg of freeze-dried tissue were ground into a fine homogeneous
227 powder under liquid nitrogen with a mortar and pestle and stored at -20°C until analyses. The
228 extraction buffer consisted of a 30:70 ethanol:water mixture acidified with hydrochloric acid (pH
229 = 2.6) to prevent oxidation. Extraction was performed at 25°C for 30 min with 0.5 mL of
230 extraction buffer under constant agitation. The extract was centrifuged and the supernatant was
231 retrieved and stored at -20°C. Total soluble phlorotannin quantification in the extracts was
232 determined using a modified Folin-Ciocalteu method (Van Alstyne et al., 1999; Zhang et al.,

233 2006). Phloroglucinol (Sigma) was used as a standard. Extracts were diluted 2 to 10 times with
234 extraction buffer for absorbance to be in the range of the standard curve. Absorbance
235 measurements were performed using multiwall plates (Nunc UV-Star 96 wells) containing 10 μL
236 of extract, 50 μL of Folin-Ciocalteu reagent (Sigma) and 40 μL of Na_2CO_3 7.5 % (m/v). Plates
237 were incubated in the dark at room temperature for 2 h. Absorbance was measured at $\lambda = 750$ nm
238 on a spectrophotometric microplate reader (Safire²Tecan Multi-detection Microplate reader). For
239 each sampling time, the cage was used as biological replicate ($n = 5$) and each sample was
240 measured in two technical replicates. Technical (measurement) replicate values were averaged
241 prior to statistical analyses. Each standard solution was run in triplicate. The concentration of
242 soluble phlorotannins within kelp fragments was calculated according to the phloroglucinol
243 standard curve and expressed in phloroglucinol equivalent in $\text{mg.g}_{\text{DM}}^{-1}$ (where DM is kelp dry
244 mass).

245 2.4.3. Carbon-nitrogen content

246 For each cage, 10 disks of 28 mm diameter were randomly cored on kelp fragments and stored at
247 -20°C until preparation and analysis. Algal samples were rinsed with freshwater to remove
248 possible epiphytes and dried at 60°C during 48 h. Dried material was ground with a mortar and a
249 pestle and powder samples were put in tin capsules before C:N analyses. Carbon and nitrogen
250 content were measured using a Flash EA 1112 CHN analyser (ThermoFinnigan) coupled with a
251 Finnigan Delta Plus mass spectrometer, via a Finnigan Con-Flo III interface. C:N data were
252 expressed as a mass ratio.

253 2.4.4. Chlorophyll fluorescence measurements

254 Fluorescence was measured to evaluate the conservation of photosynthetic capacity of algal
255 tissues. Blades were transported from the seawater tank to the laboratory inside a dark box filled
256 with seawater. All measurements were carried out 24 h after collection between 4:00 pm and 6:00
257 pm to avoid differences in physiology related to daily cycles (Edwards and Kim, 2010; Gevaert et
258 al., 2002). Visually, the degradation state of blade fragments varied with size. Fragments were
259 therefore separated in two groups according to their surface area: small (area < 25 cm²) and large
260 (area > 50 cm²) fragments. The fluorescence signals were taken from the middle of the fragments
261 for three small and three large fragments randomly selected from each cage. At each sampling
262 time, measurements were taken for the five new-blade cages collected. Fragments were dark-
263 adapted for an additional 15 min using the Dark Leaf Clip Diving-LC (Walz) to which the optical
264 fibre of the fluorometer was applied to perform the measurements. *In vivo* Chl. a fluorescence of
265 photosystem II (PSII) was measured from each fragment using an underwater pulse amplitude
266 modulated fluorometer (Diving-PAM; Heinz Walz, Effeltrich, Germany). The maximum
267 quantum yield (F_v/F_m) of PSII, here used as a proxy of physiological capacity, was measured
268 using a 0.8 s saturating light pulse of white light (2500 μmol photons.m⁻² s⁻¹). F_v represents the
269 variable fluorescence and corresponds to the difference between the minimum fluorescence yield
270 (F₀) measured under weak red modulated light and the maximal fluorescence (F_m) measured
271 following the short saturating light pulse.

272 2.4.5. Remaining biomass

273 The remaining fragments from each litterfall cage were air-dried for 1 minute and wet-weighed
274 (wet mass, WM). Samples were then dried at 60°C for at least 48 h until reaching a constant mass
275 before being reweighed (dry mass, DM). The remaining biomass was estimated by dividing the
276 final WM by the initial WM measured at the beginning of the experiment and expressed in

277 percentage of remaining biomass (%RB). To estimate the decomposition kinetics, we calculated a
278 decomposition rate with a single exponential decay model commonly used in the literature
279 (Enríquez et al., 1993; Olson, 1963). The decomposition rate (k , in day^{-1}) was calculated from the
280 change of biomass (M) over time (t , in days) since the beginning of the experiment following the
281 equation:

$$282 \quad M_t = M_0 e^{-kt}$$

283 From this equation, the half-life of fragment detritus was measured ($T_{1/2} = k^{-1} \cdot \ln(2)$, days). It
284 gives a more intuitive description of detritus turnover times (Enríquez et al., 1993). In our case,
285 M_0 corresponds to the initial percentage of remaining biomass that is equal to 100. Additionally,
286 before drying algae, frond surface was checked for reproductive tissue presence.

287 2.5. Data analysis

288 Phlorotannin concentrations and C:N contents were compared with a one-way ANOVA using
289 degradation time as fixed factor. Post-hoc comparisons were applied using Tukey's honestly
290 significant difference (HSD) tests when significant ANOVA results were found ($p < 0.05$).

291 Phlorotannin concentration data were square-root transformed prior to analysis to meet the
292 assumptions of normality (Shapiro Wilk's test, $\alpha = 0.05$) and homogeneity of variance (Levene's
293 test, $\alpha = 0.05$). Remaining biomass, litterfall cage respiration and bacterial count values were
294 compared using a non-parametric one-way analysis of variance Kruskal-Wallis H-test with
295 degradation time as fixed factor. This procedure was used for biomass data because assumptions
296 of normality and homoscedasticity were not met even after $\log(x)$ and square-root
297 transformations. For litterfall cage respiration and bacterial counts, the low number of replicates
298 ($n = 3$) at each sampling time were not amenable to parametric analyses. Bonferroni adjustment

299 and the low number of replicates precluded the detection of differences by post-hoc Dunn
300 pairwise tests. Fv/Fm data within the same litterfall cage were averaged for small and large
301 fragments prior to analysis, due to data dependency. Fv/Fm values were compared using a two-
302 way ANOVA with degradation time and fragment size as fixed factors. Given that the response
303 of the fragment size depended on degradation time, we chose a nested design. The assumption of
304 homoscedasticity was met. Although the data did not meet the assumption of normal distribution
305 of residuals (Shapiro Wilk's test, $\alpha = 0.05$), we nonetheless selected this parametric analysis
306 because the distribution of residuals was nearly normal in the histograms and the ANOVA is
307 robust to small deviations from normality (Schmider et al., 2010).

308 All statistical analyses and graphics were carried out using the freeware R statistical environment
309 (R Core Team 2019).

310 3. RESULTS

311 3.1. Environmental parameters

312 During the experiment, temperature ranged from 11.7 to 17.8 °C reflecting seasonal fluctuation
313 typically observed in the Bay of Morlaix. No lengthy strong storms were experienced during the
314 experiment, indicating that there were no long periods of low light and high RWM between
315 experimental times (Table 1).

316 3.2. Decomposition of biomass and tissue content

317 The biomass of new *L. hyperborea* blades decreased with degradation time (Kruskal-Wallis, $H =$
318 34.2 , $df = 7$, $p < 0.001$). Biomass decomposition started after 2 weeks and showed negative
319 exponential dynamics with rapid loss during the first 11 weeks and then slowing after 15 weeks
320 (Figure 2a). After 24 weeks (5.5 months), the remaining biomass represented 16.5% and 3.8% of

321 initial mass for new blades and old blades, respectively. The decomposition rate calculated with
322 the non-linear regression model was three times higher for old blades ($k = 0.0366 \text{ day}^{-1}$, $p < 0.001$,
323 $R_{\text{raw}}^2 = 0.9682$) compared with new blades ($k = 0.0107 \text{ day}^{-1}$, $p < 0.001$, $R_{\text{raw}}^2 = 0.949$),
324 corresponding to a fragment degradation half-life ($T_{1/2}$) of 18.9 and 65.0 days, respectively (Figure
325 2b). Furthermore, after 20 and 24 weeks of degradation, reproductive tissues were observed on the
326 surface of degrading new blades.

327 Tissue composition was significantly affected by degradation time (Figure 2c, 2d). Phlorotannin
328 concentration in degrading *L. hyperborea* fragments increased significantly with time ($F_{7, 32} =$
329 30.492 , $p < 0.001$). The concentration was two times higher after 11 weeks of degradation
330 compared with any time point the first 6 weeks. This increase was significant (Tukey's HSD test,
331 $p < 0.05$) except for the comparison between week 4 and 15 ($p = 0.116$, Figure 2c). The content
332 in C:N (mass ratio) was significantly affected by degradation time ($F_{7, 32} = 6$, $p < 0.001$), with the
333 ratio increasing slightly from 4.6 after 2 weeks to a maximum of 7.3 after 15 weeks of
334 degradation. The Post-hoc Tukey's HSD test showed only some differences between times within
335 the first 6 weeks and after 11 weeks. No significant differences in C:N ratio were observed
336 among sampling times after 11 weeks (Figure 2d).

337 3.3. Detritus metabolism

338 The litterfall cage respiration rate was significantly influenced by degradation time (Kruskal-
339 Wallis, $H = 15.406$, $df = 7$, $p < 0.05$, Figure 2e). Respiration dramatically decreased by a factor of
340 3 after 2 weeks of degradation; thereafter the rate did not vary from 2 to 6 weeks. A gradual
341 increase was measured starting from 11 weeks with a maximum rate after 20 and 24 weeks of
342 degradation. At the end of the experiment, the respiration rate doubled relative to the rate
343 observed between 2 and 6 weeks (Figure 2e).

344 The photosynthetic capacity (Fv/Fm) of degrading algae varied significantly across degradation
345 time ($F_{7,60} = 6.858$, $p < 0.001$) and according to fragment size ($F_{7,60} = 11.821$, $p < 0.001$) (Figure
346 2f). Under optimal conditions, Fv/Fm values range from 0.7 to 0.8 for brown algae (Bischof et
347 al., 1999) and a reduction reflects a stress response in algae (Pearson et al., 2009). In large
348 fragments, Fv/Fm remained stable (Tukey's HSD, $p > 0.05$) and high (between 0.70 and 0.76),
349 reflecting satisfactory photosynthetic capacity, whereas the Fv/Fm of small fragments was
350 affected over time. Especially after 15 weeks, Fv/Fm values decreased and were highly variable
351 (mean \pm SD; 0.43 ± 0.24 , 0.32 ± 0.15 , 0.59 ± 0.16 after 15, 20, 24 weeks, respectively, Figure 2f).

352 3.4. Fluctuations of cultivable bacteria during the degradation of *L. hyperborea*

353 Bacterial counts on Zobell agar, alginate-Phytigel and mannitol-Phytigel plates increased by 1-2
354 orders of magnitude in the first two weeks of the experiment (Figure 3), and thereafter remained
355 stable until the end of the experiment. This variation over time was found to be statistically
356 significant for counts on alginate-Phytigel (Kruskal-Wallis chi-squared = 11.697, $df = 5$, $P =$
357 0.039) and mannitol-Phytigel (Kruskal-Wallis chi-squared = 11.655, $df = 5$, $P = 0.040$) plates.
358 Furthermore, the proportion of iodine-resistant bacteria decreased with time (Kruskal-Wallis chi-
359 squared = 10.5, $df = 4$, $P = 0.033$, Fig. 3b), from 75% at the beginning of the experiment to 5%
360 after 24 weeks.

361 4. DISCUSSION

362 Understanding the kinetic and the processes of kelp fragments degradation is essential regarding
363 the quantity of organic matter exported within adjacent habitats by kelps forests. During our
364 experiment, the degradation of kelp biomass followed a classic pattern of organic matter
365 decomposition according to a simple negative exponential model, with high heterogeneity

366 between young and old *L. hyperborea* blades. Old blades showed degradation kinetics that were
367 three times faster than those of young blades. An additional study showed that stipes degrade
368 slightly faster than old blades and four times faster (data not shown) than young blades ($k =$
369 0.0425 d^{-1} , compared to $k = 0.0366 \text{ d}^{-1}$ and $k = 0.0107 \text{ d}^{-1}$ for respectively old and young blades).
370 This shows that, depending on the export process (detachment of old blades, erosion or
371 dislodgment during storms), fragments may have different residence times in coastal ecosystems.
372 The degradation of kelp organic matter thus follows two different types of patterns. The classic
373 export due to the natural kelp life cycle results in a pulse of organic matter during spring and
374 summer, and this tissue degrades relatively quickly. By contrast, material exported during storms
375 is more variable, producing slowly degrading material. Considering these accumulations or
376 drifting fragments as a transient habitat and resource for adjacent ecosystems, their influence in
377 benthic systems can be significant for several months. Surprisingly, the *L. hyperborea*
378 degradation rate appeared slow compared with other macroalgae that dominate coastal
379 ecosystems. The measured degradation rate for young *L. hyperborea* blades is 10 to 20 times
380 slower than fast growing ephemeral algal species such as *Ulva* sp. ($k = 0.34 - 0.51 \text{ d}^{-1}$) or
381 *Gracilaria* sp. ($k = 0.5 \text{ d}^{-1}$) (Conover et al., 2016), more than 5 times slower than intertidal
382 canopy-forming species such as *Fucus vesiculosus* ($k = 0.09 \text{ d}^{-1}$) (Conover et al., 2016), about 3
383 times slower than other kelp species such as *Macrocystis integrifolia* for young blades ($k = 0.032$
384 d^{-1}) (Albright et al., 1980) and similar to seagrass species ($k \approx 0.01 \text{ d}^{-1}$) (Harrison, 1989;
385 Hemminga and Nieuwenhuize, 1991) and mangrove leaves ($k = 0.011 \text{ d}^{-1}$) (Gladstone-Gallagher
386 et al., 2014). In addition, degradation dynamics may be strongly affected by seasonal patterns and
387 environmental conditions including changes in local hydrodynamics and temperature
388 fluctuations. For example, physical mechanisms certainly fragment detritus more than that
389 observed within our cages. Furthermore, our study covered the spring-summer period that

390 corresponds to late spring storms. The lower temperatures during winter likely slow down the
391 degradation process, but the high water motion during winter may speed up the process. For these
392 reasons, winter and autumn degradation kinetics are not readily predictable. Further research is
393 also needed to understand change of degradation dynamics depending on the type of recipient
394 habitat.

395 In addition to the slow degradation dynamics, photosynthetic capacity was maintained for 5.5
396 months for large fragments and for 3.5 months for small fragments. However, this capacity
397 appears to be highly variable depending on the degree of fragmentation and time of degradation.
398 Here, small fragments tended to lose their photosynthetic ability. These results have wide
399 implications for coastal ecosystem functioning, because exported detritus may continue to carry
400 out primary production and retain the energy and capacity to renew their tissues, potentially
401 explaining their partial recalcitrance to degradation. In highly hydrodynamic systems such as the
402 English Channel, this recalcitrance may increase the area of kelp forest influence and magnify the
403 impact of kelp forests on coastal and deep-sea ecosystems. Furthermore, reproductive tissues
404 were observed on degrading fragments during this six-month experiment (data not shown). The
405 persistence of reproductive tissue in drift kelp may increase the dispersal capacity of *L.*
406 *hyperborea*, partly compensating for the naturally short dispersal ranges of spores (5-200 m)
407 (Fredriksen et al., 1995).

408 Respiration showed a rapid decline at the beginning of the experiment. This early change can be
409 attributed to the capacity of kelps to modulate their metabolism depending on environmental
410 conditions (Kregting et al., 2016). Respiration increased after 11 weeks, likely reflecting the
411 metabolism of the holobiont complex formed by the degrading kelp and its associated
412 microorganisms. Degrading kelp is rapidly colonised by bacteria such as those growing on

413 alginate or mannitol, reaching an apparent maximum abundance as early as 2 weeks after
414 fragmentation.

415 Kelps possess a unique defence metabolism, associated in particular with the production of toxic
416 iodine compounds and phlorotannins (Potin et al., 2002). Iodine is highly concentrated in the
417 peripheral cell layers, creating specific niches for associated bacteria during iodovolatilisation
418 (Küpper et al., 2008; Verhaeghe et al., 2008). Our preliminary results on iodine-tolerant bacteria
419 suggest some changes in bacterial community composition. As *L. hyperborea* tissue is degrading,
420 iodine from the alga may be released in the environment, making the associated specific niches
421 disappear. Interestingly, the detected concentration of phlorotannins in degrading tissues doubled
422 after 11 weeks. This result is counterintuitive and refutes the claim that kelps quickly initiate
423 defence responses to minimise grazing pressure and stress soon after dislodgement (Norderhaug
424 et al., 2006). Instead, this apparent increase in phlorotannins may reflect the early degradation
425 stage of kelp tissue after 11 weeks. The degradation of cell walls by colonising bacteria may
426 make phlorotannins more accessible and increase the extraction efficiency during phlorotannin
427 concentration assays.

428 The C:N ratio also followed a counterintuitive trend and remained stable for 5.5 months. Previous
429 studies have shown a decrease in the C:N ratio related to the degradation of kelps, reflecting an
430 enrichment in nitrogen (Norderhaug et al., 2006; Sosik and Simenstad, 2013). Our results show
431 the opposite trend, with no change or a slight increase in C:N as previously observed by Dethier
432 et al. (2014). We suggest that, in the present experiment, kelp tissues did not degrade enough to
433 observe a decrease in C:N.

434 Our study allows a better understanding of *in situ* kelp degradation dynamics over the
435 spring/summer period. We showed that drifting *Laminaria hyperborea* have a high capacity to

436 resist degradation, maintaining photosynthesis function for 5.5 months depending on the degree
437 of fragmentation. Confirming this pattern of degradation dynamics requires testing different
438 environmental conditions (hydrodynamism, depth) and seasons in future studies. In natural
439 conditions, accumulations or marine litterfall vary over time and fragments can drift between
440 different habitats after being exported. Although these changes in environmental conditions
441 during the degradation process complicate the understanding of the impact of kelp fragments on
442 coastal ecosystems, there is no doubt that this pulse of organic matter can be used by recipient
443 ecosystem food webs.

444 ACKNOWLEDGMENTS

445 We would like to thanks the marine operation staff of Roscoff Biological Station (*Service Mer &*
446 *Observation SBR*), especially L. Levêque, Y. Fontana, W. Thomas, M. Camusat, N. Guidal and
447 F. Le Ven for their help with scuba diving fieldwork and experimental set-up. We also thank
448 Metabomer platform of Roscoff Biological Station (*FR2424*) for C:N sample analyses. This work
449 benefited from the support of the Brittany Regional Council and the French Government through
450 the National Research Agency with regards to the investment expenditure program IDEALG
451 (reference: ANR-10-BTBR-04).

452 REFERENCES

- 453 Albright, L.J., Chocair, J., Masuda, K., Valdés, M., 1980. *In situ* degradation of the kelps
454 *Macrocystis integrifolia* and *Nereocystis luetkeana* in British Columbia coastal waters. *Nat. Can.*
455 107:3-10.
- 456 Bartsch, I., Wiencke, C., Bischof, K., Buchholz, C.M., Buck, B.H., Eggert, A., Feuerpfeil, P.,
457 Hanelt, D., Jacobsen, S., Karez, R., Karsten, U., Molis, M., Roleda, M.Y., Schubert, H.,
458 Schumann, R., Valentin, K., Weinberger, F., Wiese, J., 2008. The genus *Laminaria* sensu lato :

- 459 recent insights and developments. *Eur. J. Phycol.* 43, 1–86.
460 <https://doi.org/10.1080/09670260701711376>
- 461 Bennett, S., Wernberg, T., de Bettignies, T., Kendrick, G.A., Anderson, R.J., Bolton, J.J.,
462 Rodgers, K.L., Shears, N.T., Leclerc, J.-C., Lévêque, L., Davoult, D., Christie, H.C., 2015.
463 Canopy interactions and physical stress gradients in subtidal communities. *Ecol. Lett.* 18, 677–
464 686. <https://doi.org/10.1111/ele.12446>
- 465 Bischof, K., Hanelt, D., Wiencke, C., 1999. Acclimation of Maximal Quantum Yield of
466 Photosynthesis in the Brown Alga *Alaria esculenta* under High Light and UV Radiation. *Plant*
467 *Biol.* 1, 435–444. <https://doi.org/10.1111/j.1438-8677.1999.tb00726.x>
- 468 Bustamante, R.H., Branch, G.M., Eekhout, S., 1995. Maintenance of an Exceptional Intertidal
469 Grazer Biomass in South Africa: Subsidy by Subtidal Kelps. *Ecology* 76, 2314–2329.
470 <https://doi.org/10.2307/1941704>
- 471 Cardona, L., Revelles, M., Sales, M., Aguilar, A., Borrell, A., 2007. Meadows of the seagrass
472 *Posidonia oceanica* are a significant source of organic matter for adjoining ecosystems. *Mar.*
473 *Ecol. Prog. Ser.* 335, 123–131. <https://doi.org/10.3354/meps335123>
- 474 Christie, H., Jørgensen, N.M., Norderhaug, K.M., Waage-Nielsen, E., 2003. Species distribution
475 and habitat exploitation of fauna associated with kelp (*Laminaria hyperborea*) along the
476 Norwegian coast. *J. Mar. Biol. Assoc. UK* 83, 687–699.
- 477 Conover, J., Green, L.A., Thornber, C.S., 2016. Biomass decay rates and tissue nutrient loss in
478 bloom and non-bloom-forming macroalgal species. *Estuar. Coast. Shelf Sci.* 178, 58–64.
479 <https://doi.org/10.1016/j.ecss.2016.05.018>
- 480 de Bettignies, T., Wernberg, T., Lavery, P.S., Vanderklift, M.A., Moring, M.B., 2013.
481 Contrasting mechanisms of dislodgement and erosion contribute to production of kelp detritus.
482 *Limnol. Oceanogr.* 58, 1680–1688. <https://doi.org/10.4319/lo.2013.58.5.1680>
- 483 Dethier, M.N., Brown, A.S., Burgess, S., Eisenlord, M.E., Galloway, A.W.E., Kimber, J., Lowe,
484 A.T., O’Neil, C.M., Raymond, W.W., Sosik, E.A., Duggins, D.O., 2014. Degrading detritus:
485 Changes in food quality of aging kelp tissue varies with species. *J. Exp. Mar. Biol. Ecol.* 460, 72–
486 79. <https://doi.org/10.1016/j.jembe.2014.06.010>

- 487 Edwards, M.S., Kim, K.Y., 2010. Diurnal variation in relative photosynthetic performance in
488 giant kelp *Macrocystis pyrifera* (Phaeophyceae, Laminariales) at different depths as estimated
489 using PAM fluorometry. *Aquat. Bot.* 92, 119–128. <https://doi.org/10.1016/j.aquabot.2009.10.017>
- 490 Enríquez, S., Duarte, C.M., Sand-Jensen, K.A.J., 1993. Patterns in decomposition rates among
491 photosynthetic organisms: the importance of detritus C: N: P content. *Oecologia* 94, 457–471.
- 492 Evans, S.N., Abdo, D.A., 2010. A cost-effective technique for measuring relative water
493 movement for studies of benthic organisms. *Mar. Freshw. Res.* 61, 1327.
494 <https://doi.org/10.1071/MF10007>
- 495 Filbee-Dexter, K., Scheibling, R.E., 2014. Detrital kelp subsidy supports high reproductive
496 condition of deep-living sea urchins in a sedimentary basin. *Aquat. Biol.* 23, 71–86.
- 497 Fredriksen, S., Sjøtun, K., Lein, T.E., Rueness, J., 1995. Spore dispersal in *Laminaria hyperborea*
498 (*Laminariales*, *Phaeophyceae*). *Sarsia* 80, 47–53.
499 <https://doi.org/10.1080/00364827.1995.10413579>
- 500 Gevaert, F., Creach, A., Davoult, D., Holl, A.-C., Seuront, L., Lemoine, Y., 2002. Photo-
501 inhibition and seasonal photosynthetic performance of the seaweed *Laminaria saccharina* during
502 a simulated tidal cycle: chlorophyll fluorescence measurements and pigment analysis. *Plant Cell*
503 *Environ.* 25, 859–872. <https://doi.org/10.1046/j.1365-3040.2002.00869.x>
- 504 Gladstone-Gallagher, R., Lundquist, C., Pilditch, C., 2014. Mangrove (*Avicennia marina* subsp.
505 *australasica*) litter production and decomposition in a temperate estuary. *N. Z. J. Mar. Freshw.*
506 *Res.* 48, 24–37. <https://doi.org/10.1080/00288330.2013.827124>
- 507 Gorman, D., Bajjouk, T., Populus, J., Vasquez, M., Ehrhold, A., 2013. Modeling kelp forest
508 distribution and biomass along temperate rocky coastlines. *Mar. Biol.* 160, 309–325.
509 <https://doi.org/10.1007/s00227-012-2089-0>
- 510 Harrison, P.G., 1989. Detrital processing in seagrass systems: A review of factors affecting decay
511 rates, remineralization and detritivory. *Aquat. Bot.* 35, 263–288. [https://doi.org/10.1016/0304-](https://doi.org/10.1016/0304-3770(89)90002-8)
512 [3770\(89\)90002-8](https://doi.org/10.1016/0304-3770(89)90002-8)
- 513 Hemminga, M.A., Nieuwenhuize, J., 1991. Transport, deposition and in situ decay of seagrasses
514 in a tropical mudflat area (Banc D'Arguin, Mauritania). *Neth. J. Sea Res.* 27, 183–190.
515 [https://doi.org/10.1016/0077-7579\(91\)90011-O](https://doi.org/10.1016/0077-7579(91)90011-O)

- 516 Hendricks, J.J., Boring, L.R., 1992. Litter quality of native herbaceous legumes in a burned pine
517 forest of the Georgia Piedmont. *Can. J. For. Res.* 22, 2007–2010. <https://doi.org/10.1139/x92->
518 263
- 519 Hereward, H.F.R., Foggo, A., Hinckley, S.L., Greenwood, J., Smale, D.A., 2018. Seasonal
520 variability in the population structure of a habitat-forming kelp and a conspicuous gastropod
521 grazer: Do blue-rayed limpets (*Patella pellucida*) exert top-down pressure on *Laminaria digitata*
522 populations? *J. Exp. Mar. Biol. Ecol.* 506, 171–181. <https://doi.org/10.1016/j.jembe.2018.06.011>
- 523 Iwamoto, K., Shiraiwa, Y., 2005. Salt-regulated mannitol metabolism in algae. *Mar. Biotechnol.*
524 7, 407–415. <https://doi.org/10.1007/s10126-005-0029-4>
- 525 Kloareg, B., Quatrano, R.S., 1988. Structure of the Cell Walls of Marine Algae and
526 Ecophysiological Functions of the Matrix Polysaccharides. *Ocean. Mar Biol Annu Rev* 26, 259–
527 315.
- 528 Koivikko, R., Loponen, J., Pihlaja, K., Jormalainen, V., 2007. High-performance liquid
529 chromatographic analysis of phlorotannins from the brown algae *Fucus vesiculosus*. *Phytochem.*
530 *Anal.* 18, 326–332. <https://doi.org/10.1002/pca.986>
- 531 Kregting, L., Blight, A.J., Elsässer, B., Savidge, G., 2016. The influence of water motion on the
532 growth rate of the kelp *Laminaria digitata*. *J. Exp. Mar. Biol. Ecol.* 478, 86–95.
533 <https://doi.org/10.1016/j.jembe.2016.02.006>
- 534 Krishna, M.P., Mohan, M., 2017. Litter decomposition in forest ecosystems: a review. *Energy*
535 *Ecol. Environ.* 2, 236–249. <https://doi.org/10.1007/s40974-017-0064-9>
- 536 Krumhansl, K., Scheibling, R., 2012a. Production and fate of kelp detritus. *Mar. Ecol. Prog. Ser.*
537 467, 281–302. <https://doi.org/10.3354/meps09940>
- 538 Krumhansl, K., Scheibling, R., 2012b. Detrital subsidy from subtidal kelp beds is altered by the
539 invasive green alga *Codium fragile ssp. fragile*. *Mar. Ecol. Prog. Ser.* 456, 73–85.
540 <https://doi.org/10.3354/meps09671>
- 541 Küpper, F.C., Carpenter, L.J., McFiggans, G.B., Palmer, C.J., Waite, T.J., Boneberg, E.-M.,
542 Woitsch, S., Weiller, M., Abela, R., Grolimund, D., Potin, P., Butler, A., Luther, G.W., Kroneck,
543 P.M.H., Meyer-Klaucke, W., Feiters, M.C., 2008. Iodide accumulation provides kelp with an

- 544 inorganic antioxidant impacting atmospheric chemistry. *Proc. Natl. Acad. Sci. U. S. A.* 105,
545 6954–6958. <https://doi.org/10.1073/pnas.0709959105>
- 546 Leclerc, J.-C., Riera, P., Laurans, M., Leroux, C., Lévêque, L., Davoult, D., 2015. Community,
547 trophic structure and functioning in two contrasting *Laminaria hyperborea* forests. *Estuar. Coast.*
548 *Shelf Sci.* 152, 11–22. <https://doi.org/10.1016/j.ecss.2014.11.005>
- 549 Leclerc, J.-C., Riera, P., Leroux, C., Lévêque, L., Laurans, M., Schaal, G., Davoult, D., 2013.
550 Trophic significance of kelps in kelp communities in Brittany (France) inferred from isotopic
551 comparisons. *Mar. Biol.* 160, 3249–3258. <https://doi.org/10.1007/s00227-013-2306-5>
- 552 Li, Y., Fu, X., Duan, D., Liu, X., Xu, J., Gao, X., 2017. Extraction and Identification of
553 Phlorotannins from the Brown Alga, *Sargassum fusiforme* (Harvey) Setchell. *Mar. Drugs* 15, 49.
554 <https://doi.org/10.3390/md15020049>
- 555 Ling, S.D., Scheibling, R.E., Rassweiler, A., Johnson, C.R., Shears, N., Connell, S.D., Salomon,
556 A.K., Norderhaug, K.M., Perez-Matus, A., Hernandez, J.C., Clemente, S., Blamey, L.K., Hereu,
557 B., Ballesteros, E., Sala, E., Garrabou, J., Cebrian, E., Zabala, M., Fujita, D., Johnson, L.E., 2014.
558 Global regime shift dynamics of catastrophic sea urchin overgrazing. *Philos. Trans. R. Soc. B*
559 *Biol. Sci.* 370, 20130269–20130269. <https://doi.org/10.1098/rstb.2013.0269>
- 560 Lüning, K., 1979. Growth strategies of three *Laminaria* species (Phaeophyceae) inhabiting
561 different depth zones in the sublittoral region of Helgoland (North Sea). *Mar Ecol Prog Ser* 1,
562 195–207.
- 563 Matala, J., Kellomäki, S., Nuutinen, T., 2008. Litterfall in relation to volume growth of trees:
564 Analysis based on literature. *Scand. J. For. Res.* 23, 194–202.
565 <https://doi.org/10.1080/02827580802036176>
- 566 Miller, H.G., 1984. Dynamics of nutrient cycling in plantation ecosystems. *Nutr. Plant. For. Ed.*
567 GD Bowen EKS Nambiar.
- 568 Norderhaug, K.M., Fredriksen, S., Nygaard, K., 2003. Trophic importance of *Laminaria*
569 *hyperborea* to kelp forest consumers and the importance of bacterial degradation to food quality.
570 *Mar. Ecol. Prog. Ser.* 255, 135–144.

- 571 Norderhaug, K.M., Nygaard, K., Fredriksen, S., 2006. Importance of phlorotannin content and C :
572 N ratio of *Laminaria hyperborea* in determining its palatability as food for consumers. *Mar. Biol.*
573 *Res.* 2, 367–371. <https://doi.org/10.1080/17451000600962789>
- 574 Olson, J.S., 1963. Energy storage and the balance of producers and decomposers in ecological
575 systems. *Ecology* 44, 322–331.
- 576 Ouisse, V., Migné, A., Davoult, D., 2014. Comparative study of methodologies to measure in situ
577 the intertidal benthic community metabolism during immersion. *Estuar. Coast. Shelf Sci.* 136,
578 19–25. <https://doi.org/10.1016/j.ecss.2013.10.032>
- 579 Pandey, R.R., Sharma, G., Tripathi, S.K., Singh, A.K., 2007. Litterfall, litter decomposition and
580 nutrient dynamics in a subtropical natural oak forest and managed plantation in northeastern
581 India. *For. Ecol. Manag.* 240, 96–104. <https://doi.org/10.1016/j.foreco.2006.12.013>
- 582 Pearson, G.A., Lago-Leston, A., Mota, C., 2009. Frayed at the edges: selective pressure and
583 adaptive response to abiotic stressors are mismatched in low diversity edge populations. *J. Ecol.*
584 97, 450–462. <https://doi.org/10.1111/j.1365-2745.2009.01481.x>
- 585 Pergent, G., Romero, J., Pergent-Martini, C., Mateo, M.-A., Boudouresque, C.-F., 1994. Primary
586 production, stocks and fluxes in the Mediterranean seagrass *Posidonia oceanica*. *Mar. Ecol.*
587 *Prog. Ser.* 106, 139–146. <https://doi.org/10.3354/meps106139>
- 588 Pessarrodona, A., Moore, P.J., Sayer, M.D.J., Smale, D.A., 2018. Carbon assimilation and
589 transfer through kelp forests in the NE Atlantic is diminished under a warmer ocean climate.
590 *Glob. Change Biol.* 24, 4386–4398. <https://doi.org/10.1111/gcb.14303>
- 591 Polyakova, O., Billor, N., 2007. Impact of deciduous tree species on litterfall quality,
592 decomposition rates and nutrient circulation in pine stands. *For. Ecol. Manag.* 253, 11–18.
593 <https://doi.org/10.1016/j.foreco.2007.06.049>
- 594 Potin, P., Bouarab, K., Salaün, J.P., Pohnert, G., Kloareg, B., 2002. Biotic interactions of marine
595 algae. *Curr. Opin. Plant Biol.* 5, 308–317. [https://doi.org/10.1016/S1369-5266\(02\)00273-X](https://doi.org/10.1016/S1369-5266(02)00273-X)
- 596 Rees, R.M. (Ed.), 2001. Sustainable management of soil organic matter: based upon papers
597 offered at a meeting held in Edinburgh in September 1999. CABI Pub, Wallingford.

- 598 Schmider, E., Ziegler, M., Danay, E., Beyer, L., Bühner, M., 2010. Is It Really Robust?:
599 Reinvestigating the Robustness of ANOVA Against Violations of the Normal Distribution
600 Assumption. *Methodology* 6, 147–151. <https://doi.org/10.1027/1614-2241/a000016>
- 601 Sheppard, C.R.C., Jupp, B.P., Sheppard, A.L.S., Bellamy, D.J., 1978. Studies on the Growth of
602 *Laminaria hyperborea* (Gunn.) Fosl. and *Laminaria ochroleuca* (De La Pylaie) on the French
603 Channel Coast. *Bot. Mar.* 21. <https://doi.org/10.1515/botm.1978.21.2.109>
- 604 Sosik, E., Simenstad, C., 2013. Isotopic evidence and consequences of the role of microbes in
605 macroalgae detritus-based food webs. *Mar. Ecol. Prog. Ser.* 494, 107–119.
606 <https://doi.org/10.3354/meps10544>
- 607 Steneck, R.S., Graham, M.H., Bourque, B.J., Corbett, D., Erlandson, J.M., Estes, J.A., Tegner,
608 M.J., 2002. Kelp forest ecosystems: biodiversity, stability, resilience and future. *Environ.*
609 *Conserv.* 29. <https://doi.org/10.1017/S0376892902000322>
- 610 Teagle, H., Hawkins, S.J., Moore, P.J., Smale, D.A., 2017. The role of kelp species as biogenic
611 habitat formers in coastal marine ecosystems. *J. Exp. Mar. Biol. Ecol.*
612 <https://doi.org/10.1016/j.jembe.2017.01.017>
- 613 Thomas, F., Cosse, A., Goullitquer, S., Raimund, S., Morin, P., Valero, M., Leblanc, C., Potin, P.,
614 2011. Waterborne Signaling Primes the Expression of Elicitor-Induced Genes and Buffers the
615 Oxidative Responses in the Brown Alga *Laminaria digitata*. *PLoS ONE* 6, e21475.
616 <https://doi.org/10.1371/journal.pone.0021475>
- 617 Tzetlin, A.B., Mokievsky, V.O., Melnikov, A.N., Saphonov, M.V., Simdyanov, T.G., Ivanov,
618 I.E., 1997. Fauna associated with detached kelp in different types of subtidal habitats of the
619 White Sea. *Hydrobiologia* 355, 91–100.
- 620 Van Alstyne, K.L., McCarthy, J.J., Hustead, C.L., Kearns, L.J., 1999. Phlorotannin allocation
621 among tissues of northeastern pacific kelps and rockweeds. *J. Phycol.* 35, 483–492.
- 622 Verhaeghe, E.F., Fraysse, A., Guerquin-Kern, J.L., Wu, T. Di, Devès, G., Mioskowski, C.,
623 Leblanc, C., Ortega, R., Ambroise, Y., Potin, P., 2008. Microchemical imaging of iodine
624 distribution in the brown alga *Laminaria digitata* suggests a new mechanism for its
625 accumulation. *J. Biol. Inorg. Chem.* 13, 257–269. <https://doi.org/10.1007/s00775-007-0319-6>

- 626 Vetter, E.W., 1994. Hotspots of benthic production. *Nature* 372, 47–47.
627 <https://doi.org/10.1038/372047a0>
- 628 Wesemael, B. van, Veer, M. a. C., 1992. Soil organic matter accumulation, litter decomposition
629 and humus forms under mediterranean-type forests in southern Tuscany, Italy. *J. Soil Sci.* 43,
630 133–144. <https://doi.org/10.1111/j.1365-2389.1992.tb00125.x>
- 631 Zhang, Q., Zhang, J., Shen, J., Silva, A., Dennis, D.A., Barrow, C.J., 2006. A Simple 96-Well
632 microplate method for estimation of total polyphenol content in seaweeds. *J. Appl. Phycol.* 18,
633 445–450. <https://doi.org/10.1007/s10811-006-9048-4>

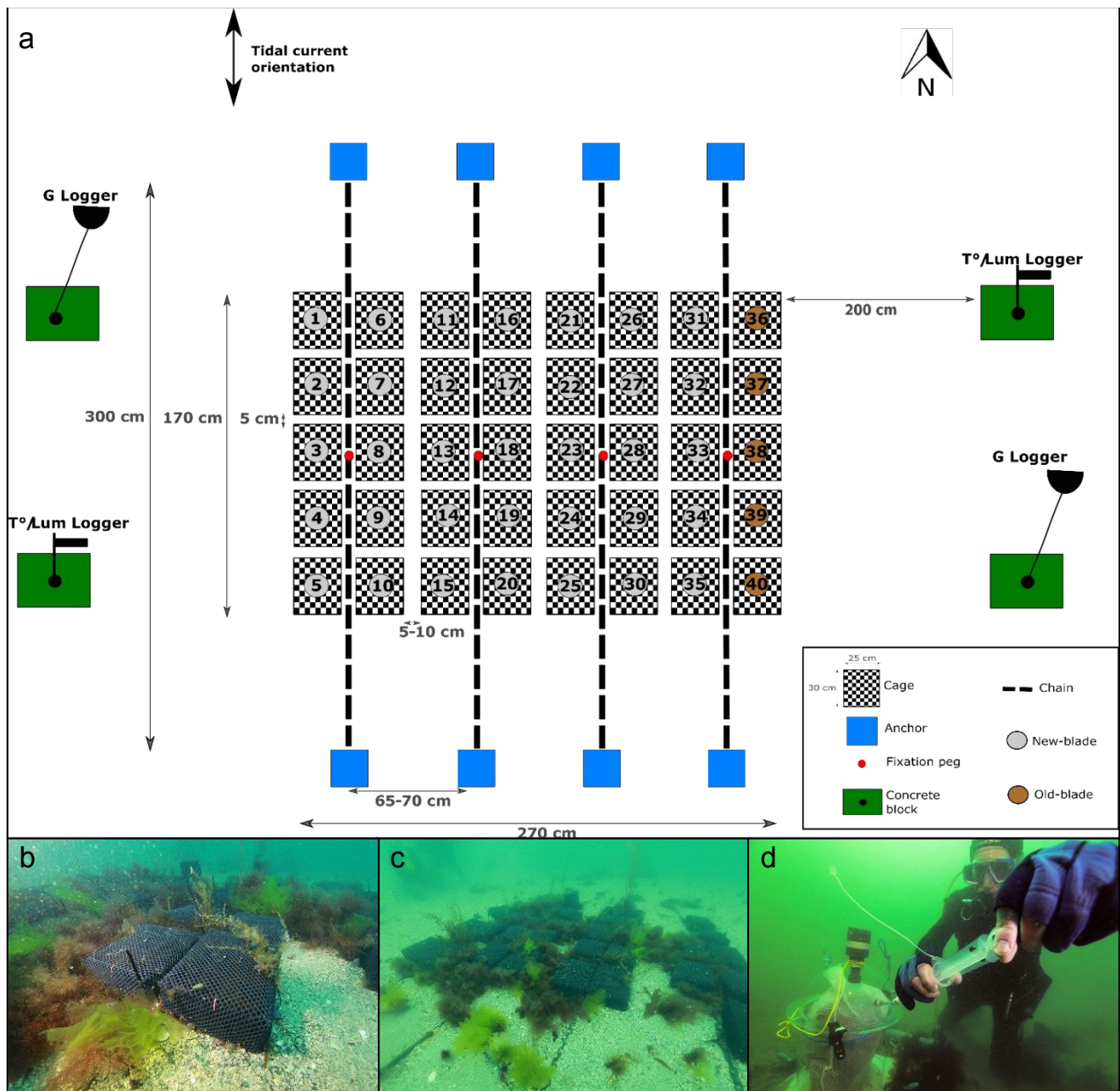


Figure 1: (a) *In situ* experimental set-up on the seabed in the Bay of Morlaix (Guerh on: 48°42'33.78" N, 003°57'12.36" W) at 9 m depth (on average). Panel (b) shows 40 custom-built plastic cages filled with 1 kg of fresh *Laminaria hyperborea* blades arranged to form an artificial accumulation of kelp fragments (c). (d) Benthic chamber incubations to estimate the holobiont respiration rates. Photographs: Wilfried Thomas, experimental schematic: Florian de Bettignies.

Table 1: Environmental parameters for each sampling time. Data provided are those measured the week before retrieval. Relative water motion data for week 20 are missing due to sensor failure.

Time (weeks)	Temperature (°C)			Light (lux)	Relative Water Motion (m.s ⁻²)		
	Mean	MinT°	Max T°	Mean	Mean	Min	Max
0	12.7	12.2	13.3	2284	0.38	0.00	1.98
2	12.3	11.7	13.7	650	0.30	0.00	2.63
4	13.4	12.6	14.5	1154	0.13	0.00	1.08
6	14.5	13.5	16.5	2260	0.25	0.00	2.02
11	15.9	15.2	17.1	956	0.33	0.00	3.08
15	16.5	15.9	17.1	272	0.22	0.00	2.27
20	17.2	16.4	17.8	199	--	--	--
24	16.1	15.9	16.4	515	0.15	0.00	1.86

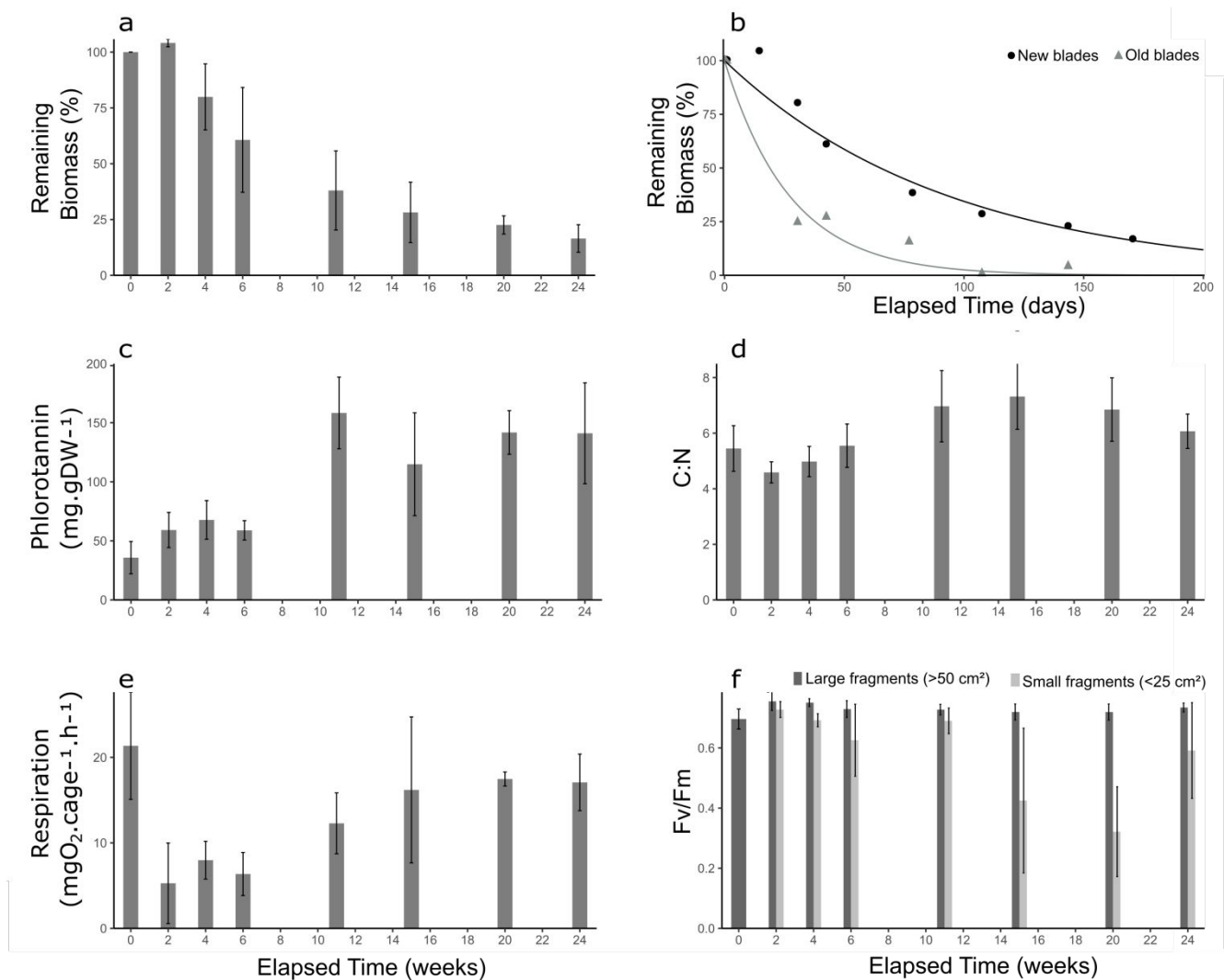


Figure 2: Parameters of degradation dynamics showing the change in (a) remaining biomass, (b) biomass decomposition models for new-blades (black circles) and old-blades (grey triangles) cages, (c) phlorotannin content, (d) C:N composition, (e) holobiont respiration rate and (f) Fv/Fm values for large (dark grey) and small (light grey) fragments. Bars give means with standard deviations ($n = 5$, except for respiration $n = 3$). Measures were taken at seven sampling times (0, 2, 4, 6, 11, 15, 20, 24 weeks). All measures are for new blades, except in panel b.

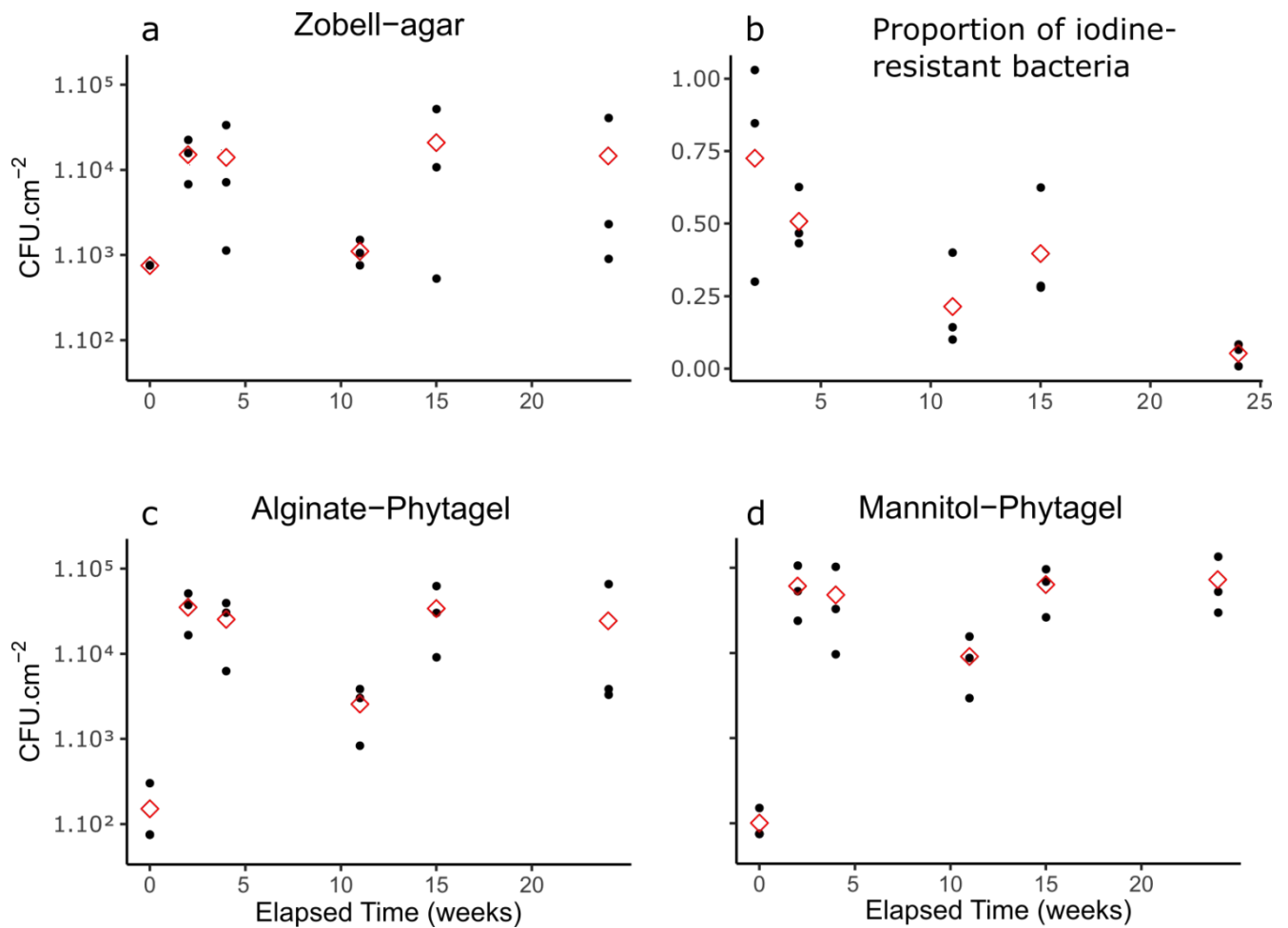


Figure 3: Cultivable bacterial counts (in number of colony-forming units per unit area of algal tissue: cfu.cm⁻²) on different growth media: (a) Zobell-agar, (b) KI-supplemented Zobell-agar, (c) alginate-Phytigel, (d) mannitol-Phytigel. Proportion of iodine-resistant bacteria was estimated as the ratio of counts obtained on KI-supplemented Zobell agar relative to the counts obtained on Zobell agar. Dots represent the raw data points from each cage replicate and the open diamonds represent the mean values.